Available at www.sciencedirect.com

ScienceDirect

journal homepage: www.elsevier.com/locate/he

Electrochemical oxidation of ammonia borane on gold electrode

*Xin-Bo Zhang, Song Han, Jun-Min Yan, Hiroshi Shioyama, Nobuhiro Kuriyama, Tetsuhiko Kobayashi, Qiang Xu**

National Institute of Advanced Industrial Science and Technology (AIST), 1-8-31 Midorigaoka, Ikeda, Osaka 563-8577, Japan

ARTICLE INFO

Article history:
Received 22 July 2008
Received in revised form
7 September 2008
Accepted 26 September 2008
Available online 21 November 2008

Keywords:
Ammonia borane
Thiourea
Cyclic voltammetry
Electrochemical oxidation
Fuel cell

ABSTRACT

The electrochemical behavior of ammonia borane on an Au electrode in the absence and presence of thiourea (TU) was detailedly investigated by cyclic voltammetry (CV). In the absence of TU, the feature of the CV is fairly complex affected by both the hydrolysis and the direct oxidation of ammonia borane. With the aid of TU, known as an effective inhibitor for the formation and recombination of adsorbed H radicals associated with ammonia borane hydrolysis, the two peaks at 414 and 0 mV may be attributed to direct electrooxidation of ammonia borane at Au electrode. These two peaks are particularly important for the practical direct ammonia borane fuel cell (DABFC). Additionally, the Tafel slope ($b = 0.15$ V) and charge transfer coefficient ($\alpha = 0.604$) were obtained as well as number of electrons exchanged ($n = 2$) in the ammonia borane oxidation at the Au/solution interface in the presence of TU.

1. Introduction

While the power demands of portable electronic gadgets – laptops, mobile telephones, iPods and the like – have exploded in the past few years, the storage capacity of the batteries used to power them has not kept pace. In a worldwide push to find alternative power sources, systems based on fuel-cell technologies, with their potentially much higher energy-storage densities, have been receiving considerable attentions [1–5]. It is now well admitted that using a liquid fuel to replace hydrogen for feeding fuel-cell anodes would have many advantages in term of their fuel-cell system simplicity, high mass and volume densities, as well as the safety reasons [6], which is mandatory for nomad electronic devices. Recently many liquid fuels, such as methanol [7–10], ethanol [11,12], and ethylene glycol [13,14], have been employed as a substitute to hydrogen for low-temperature fuel cells. However, their electrooxidations are generally slow and irreversible. Ammonia borane (NH_3BH_3), which is safe, non-toxic, chemically stable, easy to transport in its dry state and high solubility in water (stable in neutral aqueous solution), appears as an attractive fuel for fuel cells [15–22].

A novel fuel cell using the aqueous ammonia borane solution as the fuel has been proposed [23,24]. It possesses high capacity (5.2 Ahg^{-1}) and energy density (8.4 $Wh\,g^{-1}$ at 1.62 V) according to the following cell reaction:

$$NH_3BH_3 + 3/2O_2 = BO_2^- + NH_4^+ + H_2O \quad (1)$$

Moreover, the used fuel (BO_2^-) can be reverted to BH_4^- through a reaction with a saline hydride (MgH) [25]. The resultant BH_4^- can then be converted into NH_3BH_3 via a reaction in diethyl ether at room temperature [26].

* *Corresponding author*. Tel.: +81 72 751 9652; fax: +81 72 751 9629.
E-mail address: q.xu@aist.go.jp (Q. Xu).

0360-3199/$ – see front matter © 2008 International Association for Hydrogen Energy. Published by Elsevier Ltd. All rights reserved.
doi:10.1016/j.ijhydene.2008.09.083

In order to improve the performance of direct ammonia borane fuel cell (DABFC), it is of primary importance to clarify the likely oxidation mechanism for the reducing agent. However, the unwanted hydrolysis disturbs the attempts to decipher the multi-electron reactions mechanism of ammonia borane. In this case, addition of thiourea (TU) known as an effective inhibitor for H_2 evolution [27–29] is appropriate and can certainly assist us with the above mentioned problem. Thus, detailed information about the nature of gold surface in 2 M NaOH and oxidation of ammonia borane at the Au/solution interface with and without TU is urgently needed. The goal of this work is to systematically address these two questions and thereafter to determine the number of electrons transferred in the electrooxidation of ammonia borane at the Au/solution interface with aid of TU. It is expected that our results will be helpful for further confirming and understanding the direct electrooxidation of ammonia borane on Au electrode so as to help in solving the problems currently encountered in the development of DABFC with high efficiency. By addition of TU to the direct ammonia borane fuel cell, an improvement of the coulombic efficiency of DABFC by inhibiting the H_2 evolution reaction is expected.

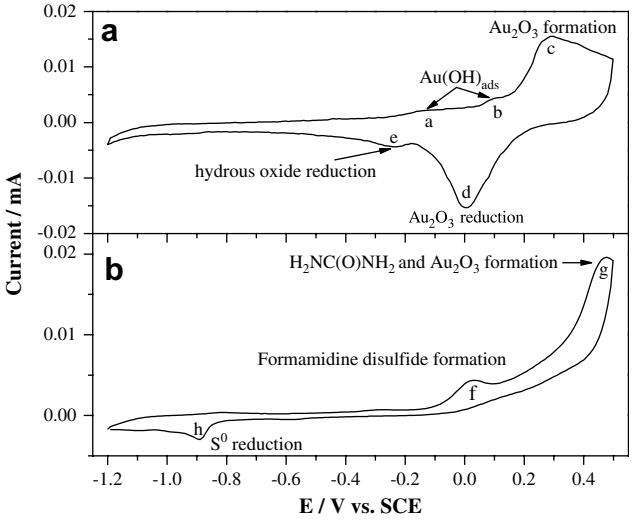

Fig. 1 – Voltammetric response (−1.2 to +0.5 V) at Au electrode in 2 M NaOH (a) without and (b) with 0.001 M CH_4N_2S at scan rate of 100 mV s^{-1}.

2. Experimental

Ammonia borane (NH_3BH_3, Aldrich, ACS Reagent, Purity 90%), sodium hydroxide (NaOH, Sigma–Aldrich, ACS Reagent, Purity 97%), thiourea (TU, CH_4N_2S, Sigma–Aldrich, ACS Reagent, Purity 100%) were used without further purification. All solutions were prepared in deionized water with a minimum resistance of 17.5 MΩ cm^{-2}. The solutions were purged with N_2 for 20 min prior to experiments in order to remover oxygen.

An Au disk with 3 mm diameter (area of 7.07×10^{-2} cm^2; BAS Inc.) was employed as the working electrode for CV tests. Before each CV experiment, the Au electrode was polished with 0.5 μm diamond paste (BAS Inc). After the mechanical pretreatment, the working electrodes were cleaned by sonication in distilled water and finally rinsed by deionized water.

Cyclic voltammograms (CV) of NH_3BH_3 on Au electrode were measured with a conventional three-electrode system using an HZ-5000 automatic polarization system (Hokuto Denko Inc., Japan). The effective cell volume was 20 ml. Pt wire was used as the counter electrode, whilst the reference electrode was a saturated calomel electrode (SCE). All experiments were performed at room temperature. Unless otherwise mentioned, all the potential values in this work are reported versus SCE.

3. Results and discussion

3.1. *Nature of gold surface in 2 M NaOH without and with TU*

The electrochemistry of an Au substrate in 2 M NaOH is shown in Fig. 1a. During the positive potential scan in the absence of dissolved O_2, charging of the double-layer region is the sole source of the small anodic current in the region from ca. −1.2 to −0.6 V. The two small anodic peaks (a and b) in excess of the charging current in the region from −0.4 to +0.2 V can be attributed to the formation of a submonolayer of adsorbed hydroxyl species $AuOH_{ads}$ which is believed to have catalytic properties for oxidation reactions of the other species in solution which involve transfer of oxygen from H_2O to their oxidation products [30,31]. The larger anodic peak (c) for E > ca. +0.2 V is the result of formation of surface oxide (Au_2O_3). During the subsequent negative scan, cathodic dissolution of Au_2O_3 produces a peak (d) at ca. 0 V, and followed by a hydrous oxide reduction peak (e).

The voltammetric response for TU in NaOH is shown in Fig. 1b. The main CV features are the three peaks at ca. +0.05 (f), +0.5 (g) and −0.9 V (h). Peak f can be attributed to the formation of formamidine disulfide [32] according to

$$2CH_4N_2S \rightarrow HN=C(NH_2)S-SC=NH(NH_2) + 2e^- + 2H^+ \quad (2)$$

Peak g commence in the potential region where peak b is observed in the Au residual response just prior to oxide formation (peak b, Fig. 1a) and hence is suspected to be catalyzed by onset of $(AuOH)_{ads}$ formation. This large anodic peak clearly dominates the voltammetric response for TU. It primarily correspond to the production of sulfate by oxidation of the sulfur in TU which has been previously adsorbed as well as that which is transported to the electrode surface simultaneously with the appearance of peak f [33]:

$$CH_4N_2S + 10OH^- \rightarrow SO_4^{2-} + H_2NC(O)NH_2 + 8e^- + 5H_2O \quad (3)$$

The oxidative detection of adsorbed and transported TU occurs simultaneously with the formation of Au_2O_3 and is concluded to occur by a catalytic mechanism in which oxygen from $(AuOH)_{ads}$ formed as an intermediate product in the generation of Au_2O_3 is transferred to the products of TU oxidation [33,34].

The final feature of note in Fig. 1b is the set of cathodic peak h obtained during the negative scan in the region from ca. −0.8 to −1.0 V. Peak h is strikingly similar to those observed in sodium sulfide solutions [35,36], and might have contributions

from adsorbed S^0 generated by incomplete oxidation of adsorbed TU [33].

3.2. Oxidation of ammonia borane at the Au/solution interface and nature of the reactive intermediate

The addition of NH_3BH_3 into the solution dramatically affects the cyclic voltammogram as shown in Fig. 2, as characterized by a number of oxidation peaks. Scanning in the positive direction, at a rate of 0.1 V s^{-1}, the first oxidation peak occurs at −931 mV (i), followed by a second anodic peak at about −442 mV (j). On the reverse scan, interestingly, an additional oxidation peak has been observed with a peak potential of 0 mV (k). Moreover, oxidation of NH_3BH_3 results in enhanced anodic current on the order of 0.5–1.3 mA, compared to 0.002–0.015 mA for Au in 2 M NaOH. Those higher current could be reasonably attributed densities to oxidation of the NH_3BH_3, perhaps via hydroxyl trihydroborate anion intermediate, BH_3OH^-, generated from reaction of NH_3BH_3 with hydroxide ion [37–39]. This intermediate may ideally oxidize at Au electrode in the base electrolyte according to the following six-electron reaction:

$$BH_3OH^- + 6OH^- \rightarrow BO_2^- + 5H_2O + 6e^- \quad (4)$$

It is reported that this direct electrooxidation of BH_3OH^- is typically observed over a wide potential range between −0.3 to −0.67 V on Au in 0.2 M KOH [40]. In the present study, the peak j is located in the same potential region, indicating that the peak j may be due to the direct electrooxidation of NH_3BH_3, probably via the intermediate BH_3OH^-, i.e., without the implication of H_2 electroxidation.

Regarding the processes responsible for the peak i, conclusions could be drawn based on the occurrence of H_2 bubble adsorbed at the Au electrode and comparison with the voltammogram obtained in the absence of NH_3BH_3 (Fig. 1a). Gyenge [29] reported that the electrooxidation of H_2 yielding from catalytic hydrolysis of BH_4^- is at the peak potentials between −0.7 and −0.9 V versus Ag/AgCl. Based on their similarity, the peak i could be attributed to the H_2/H_2O couple. The decrease of the current function ($I_{peak,i}\ \upsilon^{-1/2}$) with the increasing scan rate, together with the positive shift of the peak potential $E_{peak,i}$ with the increasing scan rate, is indicative of a C(chemical generation of H_2)-E (electrochemical oxidation of the H_2) mechanism for peak i [41–43].

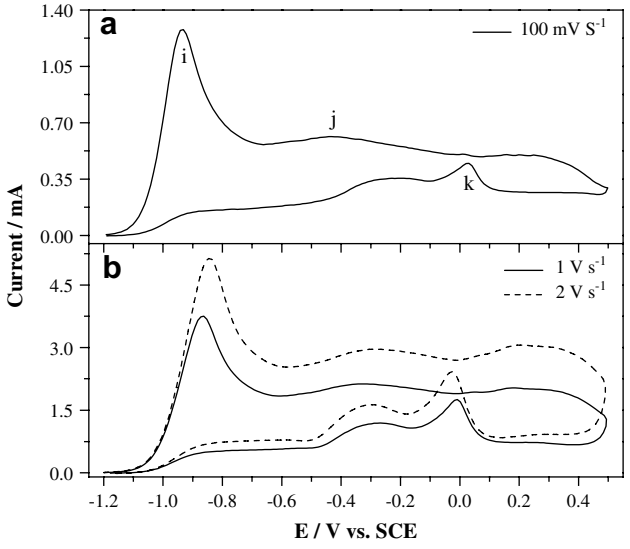

Fig. 2 – Cyclic voltammetric response of 0.01 M NH_3BH_3 in 2 M NaOH at Au electrode at different scan rates.

Accordingly, the chemical step is the hydrolysis of NH_3BH_3 yielding H_2 (Eq. (5) or (6)), followed by the electrooxidation of H_2 (Eq. (7)) (which itself is composed of either the Tafel (C)–Volmer (E) or Heyrovsky (E)–Volmer (E) steps[6]).

$$BH_3OH^- + 3H_2O \rightarrow B(OH)_4^- + 3H_2 \quad (5)$$

$$BH_3OH^- + 3OH^- \rightarrow BO_2^- + 3/2H_2 + 2H_2O + 3e^- \quad (6)$$

$$2H_2 + OH^- \rightarrow H_2O + e^- \quad (7)$$

On the subsequent cathodic sweep, there appears a sharp anodic current (peak k) due to the reactivation of the surface with respect to NH_3BH_3 oxidation. As the oxide layer is reduced in the presence of NH_3BH_3 by a local cell-type reaction with NH_3BH_3, the flow of electrons is opposite (from solution to electrode) to that normally encountered during cathodic reduction (from electrode to solution). This generates an anodic current on the cathodic scan, indicative of the behavior of a reducing agent or electron donor. The rate of oxidation in this region of the cathodic sweep was quite rapid, indicating reduction of the monolayer film gave rise to a high, but transient, coverage of adatoms, and hence hydrous oxide mediator. Oxidation ceased again at ca. −0.4 V as the mediating hydrous oxide mediator is not present at the interface at lower potentials.

3.3. Influence of thiourea on the oxidation of ammonia borane at the Au/solution interface and nature of the reactive intermediate

It is well known that thiourea (TU) has the inhibiting effect on the H_2 evolution reaction by retarding the Tafel process (i.e., $2H_{ad} \rightarrow H_2$) [41]. This effect is very important for NH_3BH_3 electrooxidation, that is, by minimizing the H_2 evolution rate, the additive could potentially improve the coulombic efficiency of DABFC. Fig. 3 shows the effect of 0.001 M TU on the NH_3BH_3 voltammogram on Au electrode in 2 M NaOH. Comparing Figs. 2 and 3, TU cancel out the voltammetric responses related to H_2 evolution in conjunction with both the catalytic hydrolysis of BH_3OH^- (reaction (5)) and the electrooxidation of BH_3OH^- (reaction (6)) responsible for peak i in Fig. 2a. The well defined peak j could be reasonably attributed to direct electrooxidation of NH_3BH_3 (via BH_3OH^- intermediate). It is noted that this reaction may be catalyzed by the Au substrate for NH_3BH_3 oxidation. Also, formation of passivating layer on the anodic scan may inhibit further NH_3BH_3 oxidation, causing a dramatic decline in current. Due to its particular importance for DABFC, this peak will be further analyzed to determine the number of electrons involved and to obtain relevant electrode kinetic parameters (vide infra). In addition, in the presence of TU one new peak k with E_{peak} at +0.276 V appears. Based on their similar potential area of peak g in Fig. 1b, this oxidation peak could also be attributed to the formation formamidine disulfide. As formation of the oxide layer nears completion (>+0.3 V), the rate of TU oxidation is

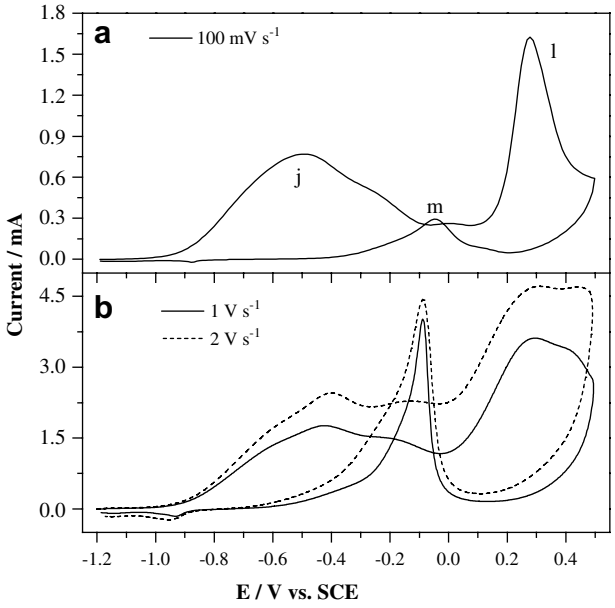

Fig. 3 – Cyclic voltammetric response of 0.01 M NH_3BH_3 in 2 M NaOH with 0.001 M CH_4N_2S present at Au electrode at different scan rates.

severely attenuated, resulting in the peak-shaped response. During the reverse scan, reduction of the gold oxide layer allows the resumption of NH_3BH_3 oxidation, giving rise to the anodic reaction peak m. Hence, because the net current during the negative scan in the region from +0.l to −0.1 V is the algebraic sum of the currents from the cathodic dissolution of Au_2O_3 and the anodic oxidation of NH_3BH_3, peak n can appear as a simple cathodic peak or a combination cathodic-anodic peak, depending on the amount of oxide being reduced, the potential scan rate v and the NH_3BH_3 flux.

3.4. *Determination of number of electrons exchanged in the electroxidation of ammonia borane at the Au/solution interface with aid of TU*

An important attempt is to determine the number of electrons exchanged (n) in the complex NH_3BH_3 electrooxidation on Au with TU present in the electrolyte and to evaluate certain kinetic parameters such as Tafel slope (b), and charge transfer coefficient (α). Values of E_{peak} for peak j (Fig. 3) obtained during the positive scan are plotted in Fig. 4 as a function of scan rates. Fig. 5 on the other hand, shows the NH_3BH_3 concentration dependence of I_{peak} of peak j (Fig. 3) at a constant scan rate (v) of 0.15 V s^{-1}. The peak current is a linear function of NH_3BH_3 concentration between 0.01 and 0.1 M (Fig. 5). The scan rate v dependence of the peak potential (E_{peak}) for an irreversible anodic wave can be expressed by [29,41,44]

$$E_{peak} = E^{o\prime} + b\left[0.52 - \frac{1}{2}\log\left(\frac{b}{D}\right) - \log k^0 + \frac{1}{2}\log v\right] \quad (8)$$

with

$$b = \frac{2.3RT}{(1-a)n_aF} \quad (9)$$

and

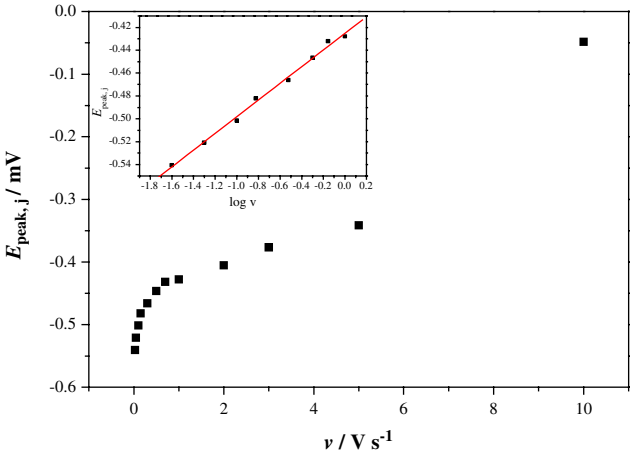

Fig. 4 – Scan rate dependence of peak j potential $E_{peak,\ j}$ for the electrooxidation of 0.01 M NH_3BH_3 on Au gold electrode in 2 M NaOH with 0.001 M thiourea (inset is $E_{peak,\ j}$ versus log v).

$$I_{peak} = (3\times10^5)n\left(\frac{2.3RT}{bF}\right)^{0.5} AC_bD^{0.5}v^{0.5} \quad (10)$$

where parameter $E^{o\prime}$ is formal potential, b is Tafel slope, D is the diffusion coefficient (8.45×10^{-6} cm^2 s^{-1}, in 2 M NaOH), k^0 is standard heterogeneous rate constant, R is universal gas constant (8.314 J mol^{-1} K^{-1}), T is the temperature (298 K), n is the total number of electron exchanged, F is the faradic constant (96,485 C mol^{-1}), A is the geometric electrode area, C_b is the bulk NH_3BH_3 concentration, and n_a is the number of electron transferred in the rate determining step. By applying equations (8) and (9), the slope of the regression line from Fig. 4 (inset) yields the Tafel slope $b = 0.15$ V and correspondingly the term $(1-\alpha)n_a = 0.396$. Based on the latter parameter, the most likely values are $n_a = 1$ and $\alpha = 0.604$.

The number of electrons exchanged n, is determined by fitting equation (10) [29] from the data shown by Fig. 5. A value of $n = 2$ has been obtained. Thus, the direct electrooxidation

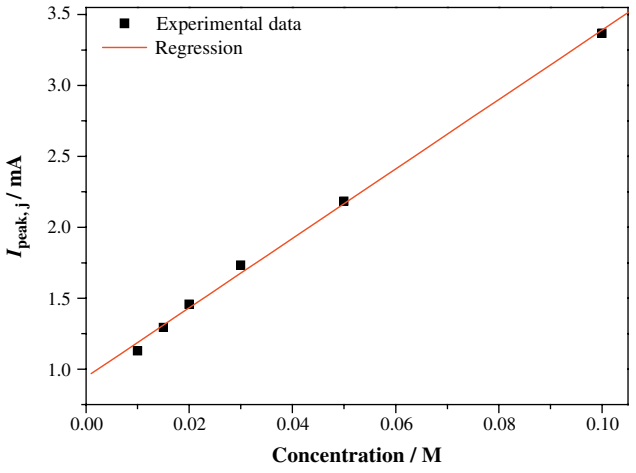

Fig. 5 – Anodic peak height of peak j at Au electrode as a function of NH_3BH_3 concentration.

of NH_3BH_3 on Au in the presence of TU is a two-electron process as opposed to the theoretical maximum of six electrons suggested by Eq. (4). Interestingly, although through the same reaction intermediate (BH_3OH^-), the electrons exchanged at gold electrode for BH_4^- and NH_3BH_3 are quite different. The significant effect of NH_4^+ on the electro-oxdiation behavior of BH_3OH^- may responsible for this difference. Further intensive studies, such as nano-particles surface modification [45–48], are needed to achieve the theoretical six electrons.

4. Summary

The electrochemical oxidation of NH_3BH_3 at Au electrode has been studied in the concentrated sodium hydroxide medium by cyclic voltammetry over a wide potential range (between -1.2 and $+5$ V versus SCE). The cyclic voltammogram on Au is fairly complex influenced by both the hydrolysis and direct oxidation of NH_3BH_3. The latter reaction occurring at potentials -414 and -0 mV is practically important for DABFC. To assist analyze this peak, TU is introduced to the solutions and expected to inhibit the H_2 evolution; therefore, it could improve the ammonia borane utilization efficiency and coulombic efficiency of DABFC. Evidenced by the present experiments, TU effectively minimizes the catalytic hydrolysis of NH_3BH_3 on Au due to the inhibiting effect of TU on the recombination of surface adsorbed hydrogen radicals. The direct oxidation of NH_3BH_3 on the other hand is favorably affected by the presence of TU (with the negative shift of potential). The issue of the long-term anode performance, stability and poisoning in the presence of TU should be considered in further studies on this topic.

Based on the experimental evidence obtained in the present work, the Tafel slope $b = 0.15$ V and charge transfer coefficient $\alpha = 0.604$ were obtained. The NH_3BH_3 oxidation in the case of the Au/TU system was determined to be a two-electron process instead of the maximum six electrons, indicating that the two-electron-loss product, $BH_2(OH)_2^-$, at this point is more stable than others. In order to gain further insights into the complex multi-electron mechanism of NH_3BH_3 oxidation on Au in the presence or absence of TU, future studies should employ coupled electrochemical and in situ detection techniques to identify the short-lived, potentially adsorbed, and reaction intermediates.

Acknowledgment

The present work is financially supported by AIST and NEDO. The authors thank Dr. Kazuaki Yasuda and Dr. Shin-ichi Yamazaki for valuable discussions.

REFERENCES

[1] Masel R. Energy technology – hydrogen quick and clean. Nature 2006;442(7102):521–2.
[2] Squadrito G, Barbera O, Giacoppo G, Urbani F, Passalacqua E. Polymer electrolyte fuel cell stack research and development. Int J Hydrogen Energ 2008;33(7):1941–6.
[3] Park JH, Shakkthivel P, Kim HJ, Han MK, Jang JH, Kim YR, et al. Investigation of metal alloy catalyst for hydrogen release from sodium borohydride for polymer electrolyte membrane fuel cell application. Int J Hydrogen Energ 2008; 33(7):1845–52.
[4] Mulder G, Coenen P, Martens A, Spaepen J. The development of a 6 kW fuel cell generator based on alkaline fuel cell technology. Int J Hydrogen Energ 2008;33(12):3220–4.
[5] Badmaev SD, Snytnikov PV. Hydrogen production from dimethyl ether and bioethanol for fuel cell applications. Int J Hydrogen Energ 2008;33(12):3026–30.
[6] Vielstich W, Lamm A, Gasteiger HA. Handbook of fuel cells: fundamentals, technology, applications. Wiley; 2003.
[7] Christensen PA, Hamnett A, Munk J, Troughton GL. An in situ FTIR study of the electrochemical oxidation of methanol at small platinum particles. J Electroanal Chem 1994;370(1–2):251–8.
[8] Tripkovic AV, Popovic KD, Grgur BN, Blizanac B, Ross PN, Markovic NM. Methanol electrooxidation on supported Pt and PtRu catalysts in acid and alkaline solutions. Electrochim Acta 2002;47(22–23):3707–14.
[9] Janssen MMP, Moolhuysen J. Binary systems of platinum and a second metal as oxidation catalysts for methanol fuel cells. Electrochim Acta 1976;21(11):869–78.
[10] Atwan M, Northwood D, Gyenge E. Evaluation of colloidal Os and Os-alloys (Os–Sn, Os–Mo and Os–V) for electrocatalysis of methanol and borohydride oxidation. Int J Hydrogen Energ 2005;30(12):1323–31.
[11] Tacconi NR, Lezna RO, Beden B, Hahn F, Lamy C. In-situ FTIR study of the electrocatalytic oxidation of ethanol at iridium and rhodium electrodes. J Electroanal Chem 1994;379(1–2):329–37.
[12] Snell KD, Keenan AG. Effect of anions and pH on the ethanol electro-oxidation at a platinum electrode. Electrochim Acta 1982;27(12):1683–96.
[13] Chang SC, Ho YH, Weaver MJ. Applications of real-time FTIR spectroscopy to the elucidation of complex electroorganic pathways – electrooxidation of ethylene-glycol on gold, platinum, and nickel in alkaline-solution. J Am Chem Soc 1991;113(25):9506–13.
[14] Kadirgan F, Beden B, Lamy C. Electrocatalytic oxidation of ethylene-glycol: part I. Behaviour of platinum ad-atom electrodes in acid medium. J Electroanal Chem 1982;136(1): 119–38.
[15] Chandra M, Xu Q. A high-performance hydrogen generation system: transition metal-catalyzed dissociation and hydrolysis of ammonia-borane. J Power Sources 2006;156(2): 190–4.
[16] Gutowska A, Li LY, Shin YS, Wang CM, Li XS, Linehan JC, et al. Nanoscaffold mediates hydrogen release and the reactivity of ammonia borane. Angew Chem Int Ed Engl 2005; 44(23):3578–82.
[17] Wolf G, Baumann J, Baitalow F, Hoffmann FP. Calorimetric process monitoring of thermal decomposition of B–N–H compounds. Thermochim Acta 2000;343(1–2):19–25.
[18] Xu Q, Chandra M. Catalytic activities of non-noble metals for hydrogen generation from aqueous ammonia-borane at room temperature. J Power Sources 2006;163(1):364–70.
[19] Chandra M, Xu Q. Dissociation and hydrolysis of ammonia-borane with solid acids and carbon dioxide: an efficient hydrogen generation system. J Power Sources 2006;159(2): 855–60.
[20] Xu Q, Chandra M. A portable hydrogen generation system: catalytic hydrolysis of ammonia-borane. J Alloy Compd 2007; 446–447:729–32.
[21] Chandra M, Xu Q. Room temperature hydrogen generation from aqueous ammonia-borane using noble metal nano-

clusters as highly active catalysts. J Power Sources 2007; 168(1):135–42.
[22] Yan J, Zhang X, Han S, Shioyama H, Xu Q. Iron-nanoparticle-catalyzed hydrolytic dehydrogenation of ammonia borane for chemical hydrogen storage. Angew Chem Int Ed Engl 2008.
[23] Zhang X-B, Han S, Yan J-M, Chandra M, Shioyama H, Yasuda K, et al. A new fuel cell using aqueous ammonia-borane as the fuel. J Power Sources 2007;168(1):167–71.
[24] Yao CF, Yang HX, Zhuang L, Ai XP, Cao YL, Lu JT. A preliminary study of direct borazane fuel cell. J Power Sources 2007;165(1):125–7.
[25] Li ZP, Liu BH, Arai K, Morigazaki N, Suda S. Protide compounds in hydrogen storage systems. J Alloy Compd 2003;356-357:469–74.
[26] Shore SG, Parry RW. The crystalline compound ammonia-borane, H3NBH3. J Am Chem Soc 1955;77(22):6084–5.
[27] Makoa T, Enyo M. The effect of surface active substances on the overpotential components of the Pd–H_2 electrode. Surface Technol 1979;9(3):147–57.
[28] Conway BE, Barber JH, Gao L, Qian SY. Effects of catalyst poisons on UPD and OPD H coverage at H_2-evolving cathodes in relation to H sorption into metals. J Alloy Compd 1997;253–254:475–80.
[29] Gyenge E. Electrooxidation of borohydride on platinum and gold electrodes: implications for direct borohydride fuel cells. Electrochim Acta 2004;49(6):965–78.
[30] Burke LD, Cunnane VJ. Involvement of incipient metal oxidation products in organic oxidation reactions at noble metal anodes. J Electrochem Soc 1986;133(8):1657–60.
[31] Vitt JE, Larew LA, Johnson DC. The importance of adsorption in anodic surface-catalyzed oxygen-transfer reactions at gold electrodes. Electroanalysis 1990;2(1):21–30.
[32] Kirchnerova J, Purdy WC. The mechanism of the electrochemical oxidation of thiourea. Anal Chim Acta 1981; 123:83–95.
[33] Vandeberg PJ, Kowagoe JL, Johnson DC. Pulsed amperometric detection of sulfur compounds: thiourea at gold electrodes. Anal Chim Acta 1992;260(1):1–11.
[34] Polta TZ, Johnson DC. Pulsed amperometric detection of sulfur compounds: part I. Initial studies of platinum electrodes in alkaline solutions. J Electroanal Chem (Lausanne Switz) 1986;209(1):159–69.
[35] Wierse DG, Lohrengel MM, Schultze JW. Electrochemical properties of sulfur adsorbed on gold electrodes. J Electroanal Chem (Lausanne Switz) 1978;92(2):121–31.
[36] Buckley AN, Hamilton IC, Woods R. An investigation of the sulphur(-II)/sulphur(0) system on bold electrodes. J Electroanal Chem 1987;216(1–2):213–27.
[37] Burke LD, Lee BH. Oxidation of some reducing agents used in electroless plating baths at gold anodes in aqueous-media. J Appl Electrochem 1992;22(1):48–56.
[38] Sargent A, Sadik OA, Matienzo LJ. Probing the mechanism of electroless gold plating using an electrochemical quartz crystal microbalance I. Elucidating the nature of reactive intermediates in dimethylamine borane. J Electrochem Soc 2001;148(4):C257–65.
[39] Iacovangelo CD. Autocatalytic electroless gold deposition using hydrazine and dimethylamine borane as reducing agents. J Electrochem Soc 1991;138(4):976–82.
[40] Okinaka Y. An electrochemical study of electroless gold-deposition reaction. J Electrochem Soc 1973;120(6):739–44.
[41] Bard AJ, Faulkner LR. Electrochemical methods. New York: Wiley; 1980.
[42] Roositer BE, Hamilton JF. Physical methods of chemistry. New York: Wiley; 1986.
[43] Brett CMA, Brett AMO. Electrochemistry: principles, methods, and applications. Oxford University Press; 1993.
[44] Gileadi E, Kirowa-Eisner E, Penciner J. Interfacial electrochemistry. Reading, MA: Addison-Wesley; 1975.
[45] Shao MH, Sasaki K, Adzic RR. Pd–Fe nanoparticles as electrocatalysts for oxygen reduction. J Am Chem Soc 2006; 128(11):3526–7.
[46] Service RF. Chemistry – platinum in fuel cells gets a helping hand. Science 2007;315(5809):172.
[47] Stamenkovic VR, Fowler B, Mun BS, Wang G, Ross PN, Lucas CA, et al. Improved oxygen reduction activity on Pt_3Ni(111) via increased surface site availability. Science 2007;315(5811):493–7.
[48] Zhang J, Sasaki K, Sutter E, Adzic RR. Stabilization of platinum oxygen-reduction electrocatalysts using gold clusters. Science 2007;315(5809):220–2.